Journal of Power Sources 196 (2011) 1258–1263

Contents lists available at ScienceDirect

Journal of Power Sources

journal homepage: www.elsevier.com/locate/jpowsour

Chromium nitride/Cr coated 316L stainless steel as bipolar plate for proton exchange membrane fuel cell

Rujin Tian*

College of Materials Science and Engineering, Dalian Jiaotong University, Huanghe Road 794, Dalian, Liaoning 116028, PR China

ARTICLE INFO

Article history:
Received 15 July 2010
Received in revised form 8 August 2010
Accepted 9 August 2010
Available online 17 August 2010

Keywords:
Bipolar plate
Stainless steel
Chromium nitride/Cr coating
Passive film
Interfacial contact resistance (ICR)

ABSTRACT

Chromium nitride/Cr coating has been deposited on surface of 316L stainless steel to improve conductivity and corrosion resistance by physical vapor deposition (PVD) technology. Electrochemical behaviors of the chromium nitride/Cr coated 316L stainless steel are investigated in 0.05 M H_2SO_4 + 2 ppm F^- simulating proton exchange membrane fuel cell (PEMFC) environments, and interfacial contact resistance (ICR) are measured before and after potentiostatic polarization at anodic and cathodic operation potentials for PEMFC. The chromium nitride/Cr coated 316L stainless steel exhibits improved corrosion resistance and better stability of passive film either in the simulated anodic or cathodic environment. In comparison to 316L stainless steel with air-formed oxide film, the ICR between the chromium nitride/Cr coated 316L stainless steel and carbon paper is about 30 mΩ cm^2 that is about one-third of bare 316L stainless steel at the compaction force of 150 N cm^{-2}. Even stable passive films are formed in the simulated PEMFC environments after potentiostatic polarization, the ICR of the chromium nitride/Cr coated 316L stainless steel increases slightly in the range of measured compaction force. The excellent performance of the chromium nitride/Cr coated 316L stainless steel is attributed to inherent characters. The chromium nitride/Cr coated 316L stainless steel is a promising material using as bipolar plate for PEMFC.

1. Introduction

Bipolar plates are one of the most important components in proton exchange membrane fuel cell (PEMFC) stacks. The traditional bipolar plates are usually fabricated from non-porous graphite. Due to its inherent brittleness and strength, the bipolar plates fabricated from graphite lead to the increases in cost, weight and volume. Therefore, metal materials are currently under consideration for using as the bipolar plate materials in PEMFC stacks. However, the metal materials are prone to electrochemical corrosion in aggressive PEMFC environments, which results in the dissolution of metallic cations and the formation of semi-conductive passive film on the surface. These factors will affect the ionic conductivity of the membrane and the power output of fuel cell stacks [1].

To overcome the formation of surface oxide and dissolution of metal in PEMFC environments, surface modification is regarded as a potential method for metal materials using as bipolar plate. Different protective coatings can be impermeable to the reactant gases and chemically inert, provide low contact resistance and offer good corrosion resistance to withstand the aggressive fuel cell environments. In many cases, the integrity of the coating can be an important issue since cracks or pinholes can lead to accelerated corrosion of the substrate. Various coatings have been used to improve the corrosion resistance or surface conductivity of metal bipolar plates, and TiN coating [2–7] and organic coatings [8–12] among of these coatings are mainly studied in the literatures.

Similar to TiN coating, chromium nitrides not only possess high electrical and thermal conductivities but also provide excellent corrosion resistance. CrN/Cr_2N coatings are considered as promising potential bipolar plate materials with excellent corrosion resistance and negligible contact resistance [13,14]. Brady et a1. [13] reported that the corrosion resistance of Ni–50Cr alloy can be improved by thermal (gas) nitridation at 1100 °C, and the ICR can be significantly decreased even after potentiostatic polarization. Since Ni–50Cr alloy is too expensive for a lot of PEMFC applications, the studies mainly focus on the thermal nitridation of stainless steels up to now. The discontinuous and porous nitride layer formed on the surface of stainless steel 349^{TM} leads to the high passive current density under both anodic and cathodic conditions [15], while nitrided AISI446 shows the lower ICR and better corrosion resistance [16]. A marked decrease in the ICR is observed for the two CrN coated stainless steels and is comparable with that of graphite [17]. Nam and Lee [18] attempted the thermal nitridation of an electroplated chromium layer on AISI316L stainless steel stainless steel and obtained the ICR value of an order of magnitude lower than that of bare AISI316L. However, the defects, such as pinhole and microcrack in CrN coating formed during preparation, can result in local corrosion. Elimination of the defects in the

* Tel.: +86 411 86933256; fax: +86 411 84106828.
E-mail address: rjtian_88@yahoo.com.cn.

0378-7753/$ – see front matter © 2010 Elsevier B.V. All rights reserved.
doi:10.1016/j.jpowsour.2010.08.028

coatings can effectively fulfill excellent corrosion resistance in the simulated PEMFC environments.

The direct deposition of CrN coating on bare steel by PVD technology appears as a simpler method than the nitridation of electro- or arc-melt deposited chromium layers. The CrN coating deposited by electron beam physical vapor deposition process not only greatly reduces the number of pinholes in the coating, but also exhibits a lower contact resistance and a higher (in the anodic environment) or similar (in the cathodic environment) corrosion resistance to the uncoated SS316L [19]. However, any pinhole in the CrN coatings can provide a site for enhancement of local corrosion, and the stainless steel substrate usually begins to corrode at the pinhole site after some period of testing. High protective efficiency of CrN coated 316L improves with decreasing bias voltage during magnetron sputtering physical vapor deposition [20]. Although Cr_xN gradient films show high interfacial conductivity and good corrosion resistance in 0.5 M H_2SO_4 + 5 ppm F^- solution, microstructure and long-term stability are not studied [21]. Cr-nitride film on 316L also shows similar properties in the simulated PEMFC environments [22]. However, the performance of this kind of bipolar plate material in actual PEMFC environment cannot be further evaluated. Good initial performance of PEMFC stacks assembled with $Cr_{0.50}Ni_{0.50}$ film coated bipolar plates is close to that of the cell assembled with the Ag-plated ones [23]. In addition, coating porosity strongly affects corrosion behavior of the coated steel. Addition of an interlayer can prevent the electrolyte solution from direct contacting the substrate steel and limiting the effect of the porosity to a great extent. For CrN/Ti multi-layered coating, the electrical resistance of the coatings depends on the bi-layer structures—Ti layer in the coatings exhibiting better electrical conductivity, and the better corrosion resistance is attributed to multi-layered coatings inhibiting the pinhole formation in the coatings [24].

In this study, the chromium nitride/Cr coating is deposited on 316L stainless steel by PVD technology. A Cr interlayer is employed to alleviate the induced stress between the substrate and chromium nitride coating. The corrosion behavior of the chromium nitride/Cr coated 316L stainless steel is investigated by electrochemical method. The interfacial contact resistance (ICR) is also evaluated before and after potentiostatic polarization at anodic/cathodic operation potential for PEMFC.

2. Experimental

In austenitic stainless steels, Cr acts as the passviating element, and Ni is a principal austenite forming/stabilizing element. Because of its higher Ni content, 316L stainless steel is considered as a baseline requirement for metallic bipolar plates. In addition, Mo is added to improve the corrosion resistance. The austenitic 316L stainless steel used in this work is a commercial plate with a thickness of 6 mm. Its typical chemical compositions (wt%) are: C < 0.030, Mn < 2.00, 16.00–18.00 Cr, 10.00–14.00 Ni, 2.00–3.00 Mo, Si < l.00, S < 0.030 and p < 0.045. The plate was solution-treated at 1000 °C for 0.5 h and then water-cooled. The specimens with area of 1 cm^2 were cut from the plate, grounded with 280–1000# abrasive paper, polished mechanically and cleaned with alcohol. High purity Cr (99.99%) target was used for different durations in high purity argon (99.99%) and nitrogen (99.99%) during deposition. As an interlayer, Cr coating was deposited precedence over chromium nitride coating. Cr and chromium nitride coatings were deposited on 316L stainless steel under total Ar + N_2 gas pressure of 0.3 Pa at 220 °C. The deposition times were 20 and 30 min, respectively. All specimens were cooled to room temperature in vacuum condition. Structure and surface morphology of modified layer were examined with XRD and SEM, respectively. XRD analysis was carried out using with Cu $K\alpha$ radiation.

Electrochemical experiments were performed using a ZAHNER IM6e potentiostat controlled by a computer. A platinum sheet and the specimen were acted as the counter and work electrode, respectively. A saturated calomel electrode (SCE) was acted as the reference electrode and contacted with the simulated solution by means of a Luggin capillary. One side of the specimen was connected to a copper wire for electrical connection. The specimens were covered with insulating epoxy and only leaving one side exposed for electrochemical measurements. The polarization curves were measured in 0.05 M H_2SO_4 + 2 ppm F^- to simulate PEMFC environments. The solution was purged either with H_2 (simulated PEMFC anodic environment) or air (simulated PEMFC cathodic environment). All electrochemical measurements were conducted at 70 °C. The specimens were stabilized in the solution at open circuit for 30 min. The cathodic polarization was conducted to eliminate the air-formed film. The scan was started in the anode direct with a scanning rate of 1 mV s^{-1}. In order to investigate the stability of the passive film formed in the simulated PEMFC environments, potentiostatic polarizations were carried out for 4 h. During the measurements, the specimens were also stabilized at open circuit for 30 min. The current density–time curves were recorded at applied anode (−0.1 V) and cathode (+0.6 V) potentials for PEMFC.

The method for measurement of the ICR between stainless steel and gas diffusion layer (carbon paper) described by Wang et al. [25] was used in this study. When an electrical current (100 mA) providing by YJ-10A type galvanostat was pass through the two copper plates, the voltage between the two copper plates was recorded. The ICR was calculated by the Ohm's law. The compaction force was applied by means of screwing a screw nut and a lead screw, and the force was recorded with a MCK-C compaction sensor and a special force gauge. The instruments and connective copper wires were unchanged during whole measurement. The calculation method of the real ICR between passive film and carbon paper has been previously described [26].

3. Results and discussion

3.1. Characterisation of coating

Fig. 1 presents XRD pattern for the chromium nitride/Cr coated 316L stainless steel. There is no peak from substrate, and the chromium nitride coating has a single fcc structure. The growth orientation of CrN is mainly in the (1 1 1) direction because the (1 1 1) peak is the strongest among these peaks. The presence of Cr peaks

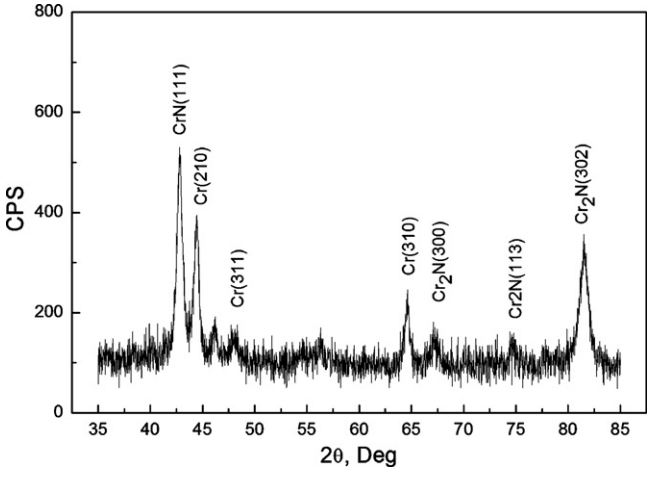

Fig. 1. XRD pattern for the chromium nitride/Cr coated 316L stainless steel.

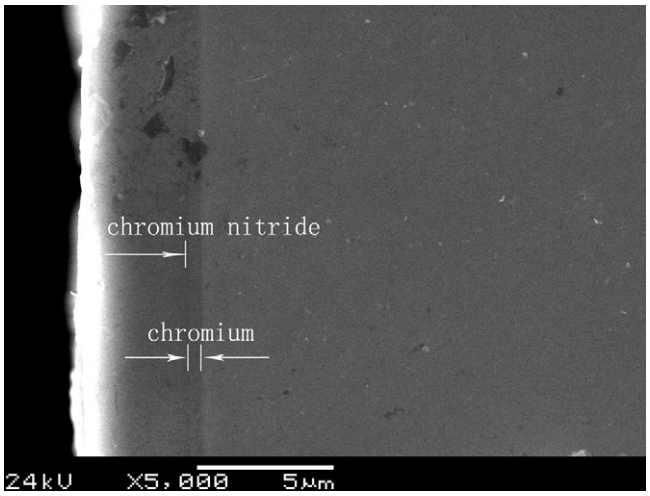

Fig. 2. Cross-sectional view of the chromium nitride/Cr coated 316L stainless steel.

shows that the chromium is not completely formed into chromium nitride during PVD deposition. A few Cr_2N peaks also present in the XRD pattern which indicates the chromium nitride coating is consisted of CrN and Cr_2N phases.

Cross-sectional view of the chromium nitride/Cr coated 316L stainless steel shows two distinct layers composed of a chromium nitride coating and a thin Cr interlayer, as shown in Fig. 2. It can be seen that the chromium nitride/Cr coating shows dense microstructure with a well-defined interface. No microcrack and void are observed in the deposited layers. The thickness of chromium nitride and Cr coatings is about 4 and 0.5 μm, respectively. Surface micrograph observed by SEM in Fig. 3 indicates that a flat and continuous chromium nitride/Cr coating has been deposited on 316L stainless steel. Some liquid droplets or microparticles scatter on the surface of the coating during deposition. The formation of the liquid droplets or microparticles may be the result of the reaction force impact of intense ion flow from the ionization region onto the specimen surface [27]. The droplets, incorporated into the coatings, can affect the properties of chromium nitride/Cr coating, in particular the corrosion resistance of the substrate 316L stainless steel. The macroparticles can lead to an increase of the coating porosity which appears to be a decisive factor in galvanic behavior with the steel substrate. No open porosity is observed in the chromium nitride/Cr coating, as shown in Figs. 2 and 3.

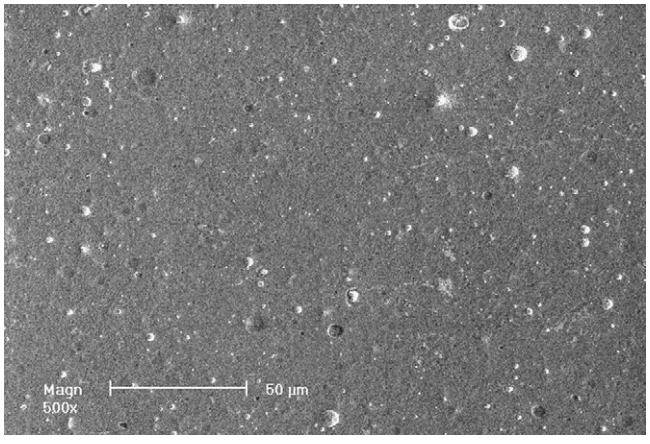

Fig. 3. SEM surface micrograph of the chromium nitride/Cr coated 316L stainless steel.

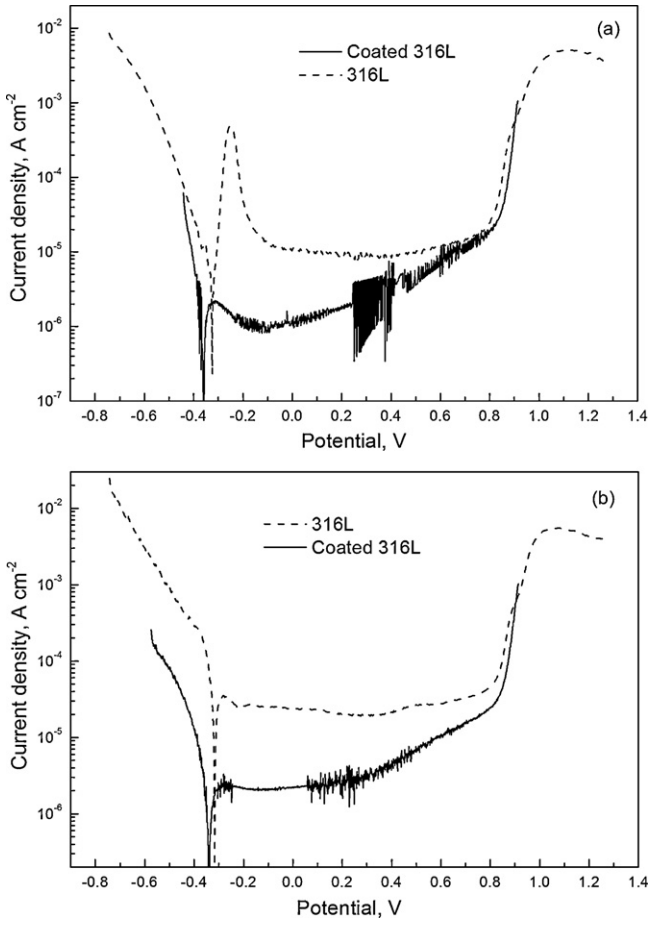

Fig. 4. Polarization curves of 316L stainless steel and the chromium nitride/Cr coated 316L stainless steel in 0.05 M H_2SO_4 + 2 ppm F^- at 70 °C. (a) purged with H_2 and (b) purged with air.

3.2. Electrochemical measurement

Fig. 4 shows the polarization curves for the as-polished and chromium nitride/Cr coated 316L stainless steel in 0.05 M H_2SO_4 + 2 ppm F^- purged with H_2/air to simulate PEMFC environments. Chromium nitride/Cr coated 316L stainless steel exhibits lower critical passive current density than 316L stainless steel either in anodic or cathodic environment, which indicates its easier passive property, as shown in Fig. 4(a) and (b). The appearance of passive current density is attributed to the formation of passive film formed on the surface. In addition, more stable passive current density of 316L stainless steel is related to its single uniform austenite phase. The chromium nitride/Cr coatings quietly decreases the passive current densities, practically no pitting is observed up to 1.6 V due to the advantages of the less defective coating surface. Because trivalent chromium is probably oxidized to hexavalent, the transpassivation occurs, and a marked increase in current density is observed. It can be seen from Fig. 4 that the passive current densities for 316L stainless steel decrease about one order of magnitude in simulated PEMFC environments due to the deposited chromium nitride/Cr coating. The passive current densities for chromium nitride/Cr coated 316L stainless steel are lower than 10 μA cm^{-2}, and meet the general target of corrosion resistance of DOE. It is worth to note that the corrosion resistance of chromium nitride/Cr coated 316L stainless steel is slightly better in the anode side than that in the cathode one. This is different from most metals which have better corrosion resistance in the cathode environment than in the anode environment due to passivation of metals [28,29].

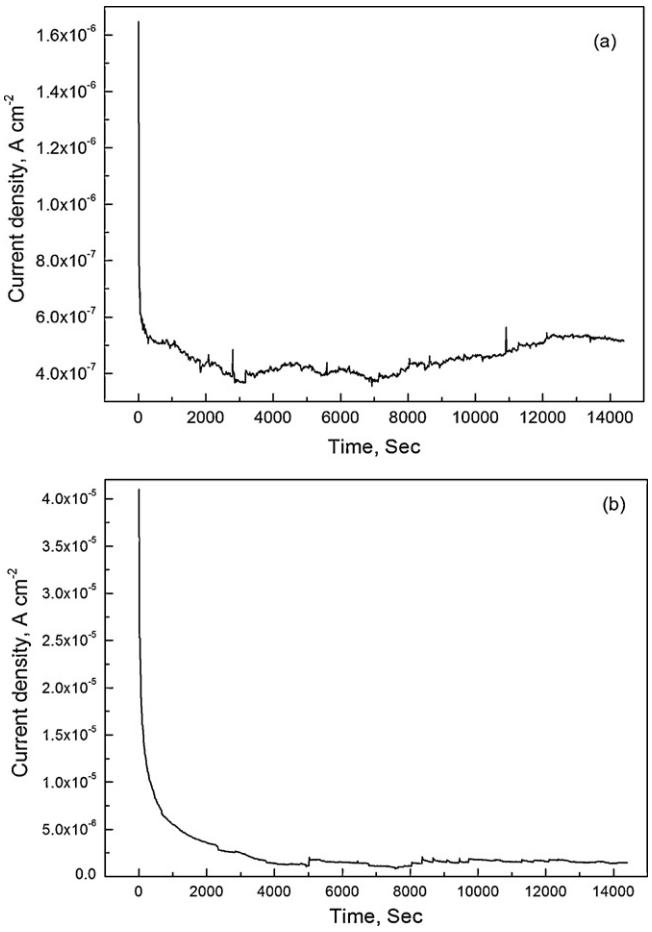

Fig. 5. Current density–time relationship of the chromium nitride/Cr coated 316L stainless steel in 0.05 M H_2SO_4 + 2 ppm F^- at 70 °C. (a) purged with H_2 at −0.1 V and (b) purged with air at +0.6 V.

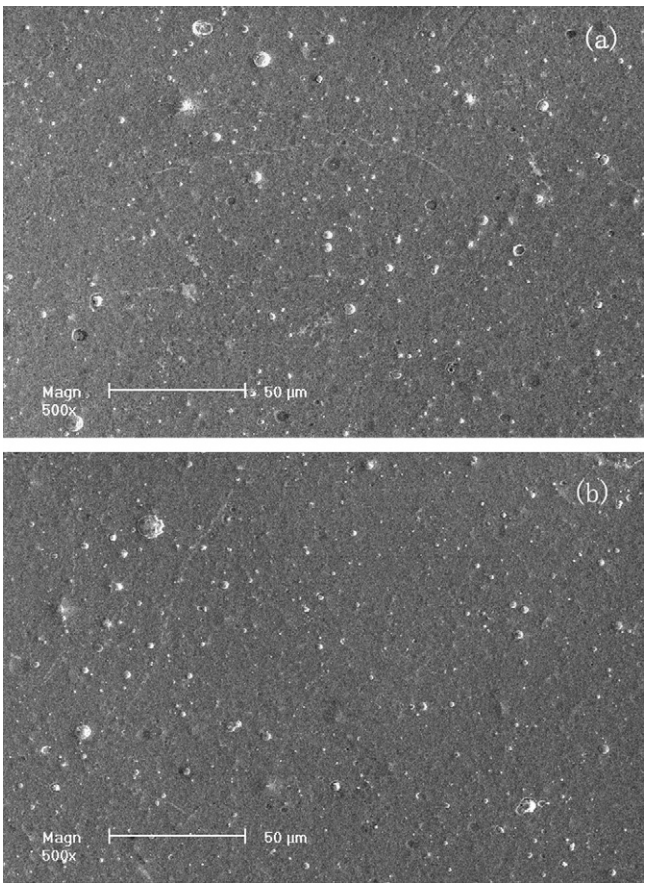

Fig. 6. Surface morphology of the chromium nitride/Cr coated 316L stainless steel after potentiostatic polarization in 0.05 M H_2SO_4 + 2 ppm F^- at 70 °C. (a) purged with H_2 at −0.1 V and (b) purged with air at +0.6 V.

The bipolar plates often operate at the anodic and cathodic operation potential for PEMFC stacks, respectively. The results of potentiostatic polarization measurements for the chromium nitride/Cr coated 316L stainless steel in 0.05 M H_2SO_4 + 2 ppm F^- simulating PEMFC environments are shown in Fig. 5(a) and (b). In both simulated PEMFC environments, the transient current density decays quite fast in the early stage, then gradually decreases, and lastly stays at a very low level. This implies that as soon as the whole surface is covered by the passive film, the current density which is necessary to maintain the passivation becomes very low. The fluctuation of transient current density maybe results from the scattered liquid droplets or microparticles on the surface during deposition. Comparison with the anodic side, the time needed for maintaining the stability of the passive film is shorter in the simulated cathodic environment for PEMFC. The lowest current density is about 5×10^{-7} A cm^{-2} in the simulated anodic side and about 1.3×10^{-6} A cm^{-2} in the cathodic one, which implies that the passive film formed on the surface of chromium nitride/Cr coated 316L stainless steel has better long-term stability in the simulated PEMFC environment. These behaviors are attributed to hydrogen oxidation in anodic side and oxygen reduction in cathodic side. Therefore, corrosion degree of the chromium nitride/Cr coated 316L stainless steel in anodic environment is slight than that in cathodic environment, which is consisted with the statement of the measurement of potentiodynamic polarization curves. That is to say, anode (−0.1 V) and cathode (+0.6 V) are all in passive region, as shown in Fig. 4(a) and (b). In addition, dissolution of oxygen in the cathodic environment also provides better passivation ability compared with the anodic environment. No pits or corrosion deposits are observed, and only general overall corrosion has taken place on the surface of the chromium nitride/Cr coated 316L stainless steel, as shown in Fig. 6. This may be related to a denser passive Cr-oxide layer on the CrN coating during the corrosion test [30]. Therefore, the large surface areas of chromium nitride/Cr coating can protect 316L stainless steel from corrosion in simulated PEMFC environments.

3.3. Interfacial contact resistance

As an important property of bipolar plate for PEMFC, the ICR has an effect on power output of the fuel cell. The ICR between the chromium nitride/Cr coated 316L stainless steel and carbon paper was measured as a function of compaction force, as shown in Fig. 7. As a baseline for metallic bipolar plate, the ICR for 316L stainless steel was also measured under the same condition and is plotted in Fig. 7. Due to the inherent character of carbon paper, the number of contact spots between the specimen and carbon paper increases rapidly when two contacting parts start to come into contact. With increasing the compaction force, the quantities of carbon–carbon and carbon–specimen contact points and the actual conductive area increase gradually, which lead to the decrease in the ICR. Therefore, the ICR for the chromium nitride/Cr coated 316L stainless steel decreases markedly at the low compaction force, and then decrease slowly. This is consistent with the results for stainless steels reported previously [15,16,25]. Especially, the ICR for the chromium nitride/Cr coated 316L stainless steel is about 30 mΩ cm^2 at the compaction force of 150 N cm^{-2}, while the ICR

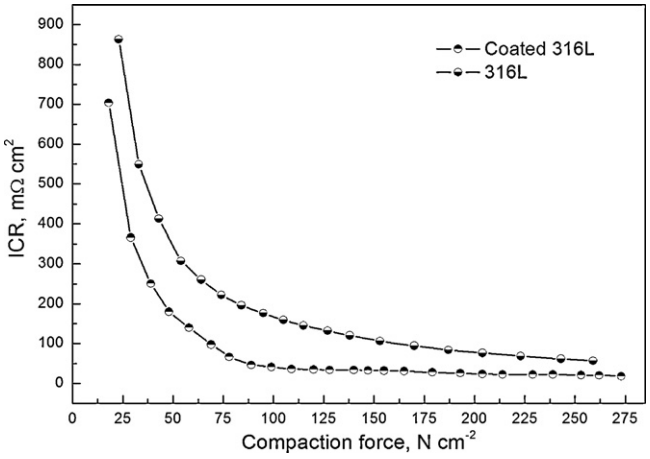

Fig. 7. ICR of the chromium nitride/Cr coated 316L stainless steel and 316L stainless steel under different compaction forces.

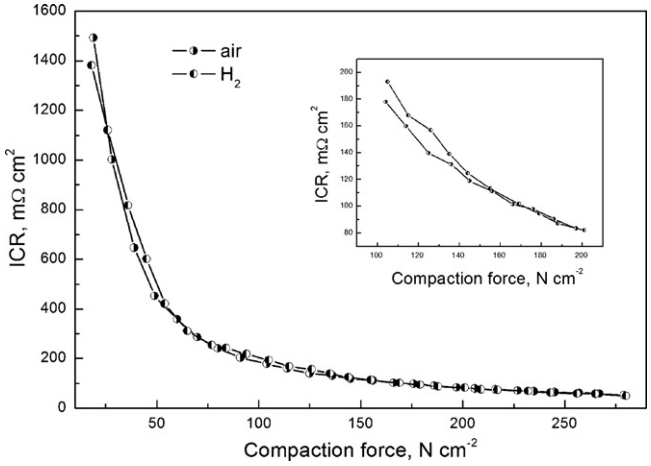

Fig. 8. ICR as a function of compaction force of the chromium nitride/Cr coated 316L stainless steel before and after potentiostatic polarization for 4 h in 0.05 M H_2SO_4 + 2 ppm F^- at 70 °C.

for 316L stainless steel is approximately 100 mΩ cm^2. It can be seen that the chromium nitride/Cr coatings deposited by PVD technology can significantly improve the surface conductivity of 316L stainless steel. The ICR of bare 316L stainless steel is higher than that of the chromium nitride/Cr coated 316L stainless steel, which can be attributed to the natural air-formed oxide film on the steel surface. It was well known that the air-formed oxide film is composed of large amount of iron oxide and Cr_2O_3. The large amount of iron oxides acting as a dopant to Cr_2O_3 have higher conductivity and lower resistance. The low contact resistance of the chromium nitride/Cr coatings results from the composition of the coating and the presence of chromium nitride phases, as shown in Fig. 1. Importantly, chromium nitride/Cr coating is conductive ceramic material with characteristic of both covalent compound and metal. In addition, as pointed out by Wang and Northwood [31], the measured ICR is higher due to larger contact area than that for the actual bipolar plate with machined flow channels fabricated from the same materials.

Once electrochemical corrosion is carried out in the simulated PEMFC environments, the passive film will formed on the surface of stainless steel bipolar plate. The chemical composition of the passive film is mainly Cr_2O_3 with the depletion of iron from film. Cr_2O_3 plays a major role on surface conductivity for the passive film, which leads to the increase in the ICR. Therefore, the conductivity of air-formed oxide film of stainless steel is superior to that of the passive film [32]. The power output of the fuel cell stacks using stainless steels as bipolar plates will decrease, and the lifetime of the stacks will not also fulfill the requirement of application. Fig. 8 shows the ICR between carbon paper and the chromium nitride/Cr coated 316L stainless steel with passive film formed in the simulated PEMFC environments under different compaction forces. The ICR decreases rapidly when the compaction force increases in a relative low level (<75 N cm^{-2}), however, when the compaction force is up to l00 N cm^{-2}, the degree of the ICR affected by compaction force is decreased, which is because the contact area between the specimen and carbon paper increase with increasing the compaction force. The ICR for the chromium nitride/Cr coated 316L stainless steel also increases over the range of applied compaction force, however, the magnitude of the increased ICR is small after 4 h potentiostatic polarization at operation potentials for PEMFC, especially in the range of the low compaction force relevant to PEMFC stacks (~100–150 N cm^{-2}). The decrease in surface conductivity results from the fact that the passive film formed on the surface of the chromium nitride/Cr coated 316L stainless steel. Moreover, it can be seen from Fig. 8 that the ICR for the passive film formed in air-purged environment at +0.6 V is almost equal to that in H_2-purged environment at −0.1 V. The simulated cathode operation condition purging with air is an oxidation environment, while the anode side purging with H_2 is a reduce environment. The effect of gas purging is not significant for the ICR of chromium nitride/Cr coated 316L stainless steel in both simulated environments.

As mentioned above, the passive film of stainless steel is mainly Cr_2O_3 with the depletion of iron from film. The Cr_2O_3 compound belongs to ionic oxide, and the electric conductivity is poor for its ionic bonding. For chromium nitride/Cr coated 316L stainless steel, the Cr_2O_3 of passive film formed on the surface of stainless steel is replaced by chromium nitride/Cr coating. The deposited chromium nitride/Cr coating contributes to the improvement in the ICR after the potentiostatic polarization in simulated PEMFC environments. Oxygen incorporation into the surface is observed in the form of increased amounts of the Cr–O species and an increased level of O in the Cr–N–O species, and the oxygen incorporation on polarization does not detrimentally affect the electrical properties of the nitrided surface [33,34]. The ICR measured after potentiostatic polarization at operation potential for PEMFC depends mainly on the inherent surface conductivity of chromium nitride/Cr coating.

Therefore, the chromium nitride/Cr coated 316L stainless steel exhibits improved corrosion resistance and high surface conductivity under PEMFC operating environments. The chromium nitride/Cr coated 316L stainless steel can be acted as a promising bipolar plate material for application in PEMFC.

4. Conclusion

Dense chromium nitride/Cr coating about 4.5 μm thick has been deposited on 316L stainless steel by PVD technology. Electrochemical behaviors and ICR measurement have been evaluated to meet the requirements of bipolar plate material for PEMFC. The lower passive current density for the chromium nitride/Cr coated 316L stainless steel in 0.05 M H_2SO_4 + 2 ppm F^- simulating PEMFC environment is in the range of 1–10 μA cm^{-2}, which is about one order of magnitude lower than that of bare 316L stainless steel. Moreover, the chromium nitride/Cr coated 316L stainless steel exhibits the stable transient current density at anodic and cathodic operation potentials, which indicates better stability of the passive film formed in simulated PEMFC environments. The SEM results indicate that the chromium nitride/Cr coated 316L stainless steel only undergoes general overall corrosion. The chromium nitride/Cr coated 316L stainless steel possesses a much lower ICR value than that of bare 316L stainless steel in the range of the measured com-

paction force. Slight increase in the ICR results from the stable passive film formed on the surface of the chromium nitride/Cr coated 316L stainless steels after potentiostatic polarization at operation potentials for PEMFC, however, it depends mainly on the inherent surface conductivity of chromium nitride/Cr coating. Based on the results presented above, the chromium nitride/Cr coated 316L stainless steel can be acted as a promising bipolar plate material for application in PEMFC.

References

[1] J. Wind, R. Spah, W. Kaiser, G. Bohm, J. Power Sources 105 (2002) 256–260.
[2] Y. Wang, D.O. Northwood, J. Power Sources 191 (2009) 483–488.
[3] N.D. Nam, J.G. Kim, W.-S. Hwang, Thin Solid Films 517 (2009) 4772–4776.
[4] E.A. Cho, U.-S. Jeon, S.-A. Hong, I.-H. Oh, S.-G. Kang, J. Power Sources 142 (2005) 177–183.
[5] Y. Wang, D.O. Northwood, J. Power Sources 165 (2007) 293–298.
[6] S.-T. Myung, M. Kumagai, R. Asaishi, Y.-K. Sun, H. Yashiro, Electrochem. Commun. 10 (2008) 480–484.
[7] W.-S. Jeon, J.-G. Kim, Y.-J. Kim, J.-G. Han, Thin Solid Films 516 (2008) 3669–3672.
[8] Y. Wang, D.O. Northwood, Thin Solid Films 516 (2008) 7427–7432.
[9] S. Joseph, J.C. McClure, P.J. Sebastian, J. Moreira, E. Valenzuela, J. Power Sources 177 (2008) 161–166.
[10] Y.J. Ren, C.L. Zeng, J. Power Sources 182 (2008) 524–530.
[11] Y. Wang, D.O. Northwood, J. Power Sources 185 (2008) 226–232.
[12] M.A. Lucio García, M.A. Smit, J. Power Sources 158 (2006) 397–402.
[13] B.P. Brady, K. Weisbrod, C. Zawodzinski, I. Paulauskas, R.A. Buchanan, L.R. Walker, Electrochem. Solid-State Lett. 5 (2002) 245–247.
[14] B.P. Brady, B. Yang, H. Wang, J.A. Turner, K.L. More, M. Wilson, JOM 8 (2006) 50–57.
[15] H. Wang, B.P. Brady, G. Teeter, J.A. Turner, J. Power Sources 138 (2004) 86–93.
[16] H. Wang, B.P. Brady, K.L. More, H.M. Meyer III, J.A. Turner, J. Power Sources 138 (2004) 79–85.
[17] A. Pozio, F. Zaza, A. Masci, R.F. Silva, J. Power Sources 179 (2008) 631–639.
[18] D.-G. Nam, H.-C. Lee, J. Power Sources 170 (2007) 268–274.
[19] L. Wang, D.O. Northwood, X. Nie, J. Housden, E. Spain, A. Leyland, A. Matthews, J. Power Sources 195 (2010) 3814–3821.
[20] N.D. Nam, J.-G. Kim, Jpn. J. Appl. Phys. 47 (2008) 6887–6890.
[21] Y. Fu, M. Hou, G. Lin, J. Hou, Z. Shao, B. Yi, J. Power Sources 176 (2008) 282–286.
[22] Y. Fu, G. Lin, M. Hou, B. Wu, H. Li, L. Hao, Z. Shao, B. Yi, Int. J. Hydrogen Energy 34 (2009) 453–458.
[23] B. Wu, Y. Fu, J. Xu, G. Lin, M. Hou, J. Power Sources 194 (2009) 976–980.
[24] W.-Y. Ho, H.-J. Pan, C.-L. Chang, D.-Y. Wang, J.J. Hwang, Surf. Coat. Technol. 202 (2007) 1297–1301.
[25] H. Wang, M.A. Sweikart, J.A. Turner, J. Power Sources 115 (2003) 243–251.
[26] R. Tian, J. Sun, L. Wang, Int. J. Hydrogen Energy 31 (2006) 1874–1878.
[27] H.-P. Feng, C.-H. Hsu, J.-K. Lu, Y.-H. Shy, Mater. Sci. Eng. A 347 (2003) 123–129.
[28] M.C. Li, C.L. Zeng, S.Z. Luo, J.N. Shen, H.C. Lin, C.N. Cao, Electrochem. Acta 48 (2003) 1735–1741.
[29] S.-J. Lee, C.-H. Huang, J.-J. Lai, Y.-P. Chen, J. Power Sources 131 (2004) 162–168.
[30] S. Rudenja, C. Leygraf, J. Pan, P. Kulu, E. Talimets, V. Mikli, Surf. Coat. Technol. 114 (1999) 129–136.
[31] Y. Wang, D.O. Northwood, Adv. Mater. Res. 41/42 (2008) 469–475.
[32] H. Wang, G. Teeter, J. Turner, J. Electrochem. Soc. 152 (2005) B99–B104.
[33] M.P. Brady, K. Weisbrod, I. Paulauskas, R.A. Buchanan, K.L. More, H. Wang, M. Wilson, F. Garzon, L.R. Walker, Scripta Mater. 50 (2004) 1017–1022.
[34] H. Wang, M.P. Brady, G. Teeter, J.A. Turner, J. Power Sources 138 (2004) 86–93.